

## A single semi-analytical algorithm to retrieve chlorophyll-a concentration in oligo-to-hypereutrophic waters of a tropical reservoir cascade

Luiz Rotta <sup>a,\*</sup>, Enner Alcântara <sup>b</sup>, Edward Park <sup>c</sup>, Nariane Bernardo <sup>a</sup>, Fernanda Watanabe <sup>a</sup>

<sup>a</sup> São Paulo State University – Unesp, Department of Cartography, Brazil

<sup>b</sup> São Paulo State University – Unesp, Department of Environmental Engineering, Brazil

<sup>c</sup> National Institute of Education and Asian School of the Environment, Nanyang Technological University, Singapore



### ARTICLE INFO

**Keywords:**  
 OLI/Landsat-8  
 Tietê River Cascade System  
 Trophic state  
 Quasi-Analytical Algorithm  
 Absorption coefficient

### ABSTRACT

Previous studies have shown the challenges in using a single model to estimate chlorophyll-a concentration (Chl-a) in water bodies with widely differing characteristics. A single model based on remote sensing to map the Chl-a distribution across the entire Tietê River Cascade System (TRCS) serves as a cost and time-efficient alternative to the conventional monitoring by providing trophic status over space and time. The Tietê River contains one of the largest cascade reservoir systems in the world, which sustains important ecological and socio-economic activities in the São Paulo State, Brazil. Surplus nutrients in water draining its surrounding catchments have been the main cause of eutrophication in the reservoirs of the TRCS. To assess the trophic state of the reservoirs, Chl-a has been regularly monitored by sampling points. However, they are limited by operational costs and dependent on weather conditions. Moreover, the current sampling method only produces point-based measurements. In this paper, we calibrate remote sensing images based on the absorption coefficient to map the spatial distribution patterns of Chl-a levels in the reservoirs. Mapping is done by estimating the Chl-a concentration. The absorption coefficients were retrieved from OLI/Landsat images using the Quasi-Analytical Algorithm (QAA). The total absorption ( $a_t$ ) in 482 nm and 655 nm retrieved by QAA presented NRMSE of 17% and 18.5%, respectively. Both  $a_t$  (482 and 655 nm) were used in the model calibration and presented a satisfactory result covering all data ranges, with  $R^2$  of 0.646 and NRMSE of 15.3%. The proposed model in this study to retrieve Chl-a maps with relatively high accuracy can be incorporated into the operational monitoring system of the TRCS at a low cost that can provide timely information for reservoir managers to carry out necessary actions. This may include mitigating environmental impacts caused by sudden algae blooms.

### 1. Introduction

The Tietê River, composed of six hydroelectric reservoirs in the São Paulo State: Barra Bonita (BB), Bariri (BAR), Ibitinga (IBI), Promissão (PR), Nova Avanhandava (NAV) and Três Irmãos, is one of the largest reservoir cascade in the world. It stores about 29 billion m<sup>3</sup> of water (AES, 2020; FURNAS, 2020). According to Tundisi et al. (1991), this cascade of reservoirs is both ecologically and socio-economically crucial. It not only provides nutrient and phosphorous necessary to sustain the aquatic communities and houses rich biodiversity (Tundisi et al., 2008; Padisák et al., 2000), but also supplies water to the extensive agricultural, industrial sectors and large population in the São Paulo State (Ussami and Guilhoto, 2018; Soares et al., 2017; Rodrigues et al., 2014). Therefore, management of the water quality in the reservoirs

along the Tietê River is a critical issue to the local populations. Satellite and *in situ* remote sensing have been effectively used to monitor the water quality in the Tietê River Cascade System (TRCS) by quantifying parameters such as chlorophyll-a (Chl-a) (Andrade et al., 2019; Watanabe et al., 2019, 2016), suspended particulate matter (SPM) (Bernardo et al., 2019a, 2016; Rodrigues et al., 2017a), colored dissolved organic matter (CDOM) (Watanabe et al., 2018; Alcântara et al., 2016a), and aquatic vegetation (Rotta et al., 2018, 2019).

The increase in the nutrient loadings has been identified as the primary cause of eutrophication in many reservoirs worldwide (e.g. He et al., 2011; Karadžić et al., 2010; Kim et al., 2001; Smith et al., 1999; Tundisi et al., 1993). In case of the Barra Bonita reservoir in the TRCS, the increase in eutrophication during the last 20 years has adversely affected the primary productivity of phytoplankton, the

\* Corresponding author.

E-mail addresses: [lh.rott@unesp.br](mailto:lh.rott@unesp.br), [luizhrotta@gmail.com](mailto:luizhrotta@gmail.com) (L. Rotta).

bacterioplankton and zooplankton communities, as well as the trophic structure in Barra Bonita reservoir (Tundisi et al., 2008). The main source of the surplus nutrients into the Tietê reservoirs include point sources, such as industrial and domestic sewage, and diffuse sources from agricultural activities (Abe et al., 2009; Rodghe et al., 2005; Tundisi et al., 1991). According to Kirk (2011), the concentration of photosynthetic pigments (such as chlorophylls) in the waterbody can be affected by environmental variables such as nitrogen concentration and light availability. For that, the Chl-a has been considered as a proxy to directly identify the trophic state in several reservoirs around the world (Yoon et al., 2019; Zhang et al., 2016, 2009; Watanabe et al., 2015). Mapping Chl-a concentration, therefore, can inform water resources managers in controlling the reservoir flows, intervening with actions to prevent and mitigate its environmental, economic, and social effects.

Empirical and semi-empirical models based on reflectance from remote sensing data have been used to map the Chl-a concentration in inland waters (Watanabe et al., 2019; Bohn et al., 2018; Duan et al., 2010; Dall'Olmo and Gitelson, 2005; Kallio et al., 2003; Oki and Yasuoka, 2002). Empirical models based on OLI/Landsat-8 to estimate Chl-a and trophic state of Barra Bonita reservoir were evaluated by Watanabe et al. (2015). Watanabe et al. (2015) demonstrated that several calibrations proposed in the literature did not obtain satisfactory results for Barra Bonita, and they suggested a further investigation of other approaches, such as semi-analytical and QAA to estimate Chl-a. Cairo et al. (2020) proposed a hybrid approach to estimate Chl-a in the Ibitinga reservoir. They verified that the algorithms applied to estimate Chl-a have better performance when calibrated for a specific Chl-a range. The development of the hybrid approach has been limited to the data used in the study and it was suggested that aquatic systems with different conditions should be incorporated into the dataset to be more representative of tropical regions (Cairo et al., 2020). The Chl-a in a cascading reservoir (Barra Bonita, Bariri and Ibitinga) was estimated based on spectral indexes on MSI/Sentinel-2 images (Watanabe et al., 2019). According to Lee et al. (2002), empirical algorithms are normally appropriate for waters with optical characteristics similar to those used in the algorithm development. This limits applicability to different water types and can result in significant errors. To overcome this limitation, Lee et al. (2002) proposed the Quasi-Analytical Algorithm (QAA), which was developed to retrieve the absorption ( $a$ ,  $m^{-1}$ ) and backscattering ( $b_b$ ,  $m^{-1}$ ) coefficients from remote sensing reflectance ( $R_{rs}$ ,  $sr^{-1}$ ) of optically deep waters (Lee et al., 2002).  $a$  and  $b_b$  are the most significant factors affecting light propagation through the water columns, playing indispensable roles in the estimation of aquatic biomass, primary production, and carbon pools (Li et al., 2013). According to Mishra et al. (2014), the advantage of the QAA is that it does not require spectral models of the absorption coefficient of phytoplankton, non-algal particulates, and CDOM ( $a_{\phi}$ ,  $a_{NAP}$ , and  $a_{CDOM}$ , respectively) for the derivation of total absorption ( $a_t$ ).

According to Li et al. (2013), the development of a model for estimating inherent optical properties (IOPs) and Chl-a is important for understanding the bio-optical properties and occurrence of algal blooms in eutrophic reservoirs, lakes and estuaries. They first proposed a model to estimate Chl-a based on absorption coefficients that resulted in  $R^2$  of 0.929 and mean relative error of 21.65%, using the samples collected across eight different reservoirs over different seasons. Le et al. (2009) calibrated and validated a QAA for the highly turbid water of Taihu Lake in the lower Yangtze River in China. They suggested that the seasonal and regional remote sensing data are necessary for using the QAA algorithm in different optical property waters.

The Operational Land Imager (OLI) onboard Landsat-8 has been previously used to retrieve IOPs using QAA. Lee et al. (2016) first used OLI data to estimate the Secchi-disk depth relied on absorption and backscattering coefficients using QAA over a turbid estuarine area. They found that the spectral resolution of the OLI bands Landsat-8 was adequate for the estimation of the Secchi-disk depth in Jialongjiang River estuary, in China. Rodrigues et al. (2017b) evaluated the

performance of deriving the Secchi-disk depth using a semi-analytical scheme based on QAA and OLI/Landsat-8 bands. A QAA-based model was parameterized by Alcântara et al. (2016b) to estimate the SPM concentration using the OLI/Landsat-8 in the Itumbiara hydroelectric reservoir in Brazil.

A few studies have used QAA based on Landsat data to estimate Chl-a concentration in inland waters. However, it has been reported that the lack of a 412 nm band restrains the use of this sensor for the analytical derivation of light absorption coefficients for phytoplankton, CDOM, and detritus (Wei et al., 2019). Furthermore, QAA parameterization of one aquatic environment may not be suitable for use in another environment where general optical characteristics are different. Existing and re-parameterized QAA versions were assessed by Andrade et al. (2019) to obtain Chl-a concentration in Ibitinga Reservoir through models based on absorption coefficients (Watanabe et al., 2016; Le et al., 2013), derived of two, three and four bands, and Normalized Difference Chlorophyll Index (NDCI) indexes (Le et al., 2013; Mishra and Mishra, 2012; Gitelson et al., 2008). QAA versions re-parameterized for other reservoirs in the same cascading system such as Nova Avanhandava (Rodrigues et al., 2018) and Barra Bonita (Watanabe et al., 2016) were not suitable for Ibitinga. According to Rodrigues et al. (2020), BB can be considered phytoplankton-dominated water while NAV was inorganic matter-dominated water. The different optical and biogeochemical characteristics between the reservoirs does not allow for the use of a single estimation model (Andrade et al., 2019). Therefore, the use of a single model to estimate Chl-a concentration in water bodies with very different environment characteristics is still a challenge and it can bring significative contributions to the monitoring of trophic status in inland waters by remote sensing, especially in large cascading reservoir systems, such as TRCS.

In this paper, we demonstrate the use of IOPs, such as the absorption coefficient, in modeling Chl-a concentration that can be applied in the entire TRCS. Our main objective, therefore, is to calibrate an IOP-based model to estimate the Chl-a concentration of the reservoirs from the TRCS. For that, IOPs were retrieved from OLI/Landsat images using QAA. Our research also presents inaugural suitability of a single semi-analytical model to retrieve Chl-a concentration for a cascade of reservoirs with widely differing limnological characteristics. Another novel aspect of our approach is the use of OLI data, which has limited spectral resolution. We found that the absorption coefficient retrieved from OLI using QAA provided results with sufficient accuracy to be used in the Chl-a model calibration for the entire cascade.

Although the State of São Paulo Environmental Company (CETESB) regularly monitors the Chl-a concentration through sampling in the reservoirs in TRCS, field sampling is often limited by the operational cost and dependent on weather conditions. Therefore until now the trophic state could be assessed only in part of the TRCS based on a few point-based samples, and obtaining spatially distributed information on the trophic state overtime remains a challenge. Therefore, a single model based on remote sensing to map the Chl-a distribution across the entire reservoir cascade will be an efficient alternative to the conventional monitoring by providing the trophic status over space and time (even in a near-real-time). We expect that our findings can be readily incorporated into the operational monitoring system of the TRCS at a low cost. It can also provide timely information to reservoir managers to execute necessary actions such as mitigating environmental impacts caused by an algae bloom.

## 2. Materials and methods

### 2.1. Study area and field campaign

Sampling points were selected in seven field campaigns across the Nova Avanhandava (NAV), Ibitinga (IBI), Bariri (BAR), Barra Bonita (BB) reservoirs (Fig. 1). At each sampling point, radiometric data and water samples were collected. A total of 120 samples were collected for

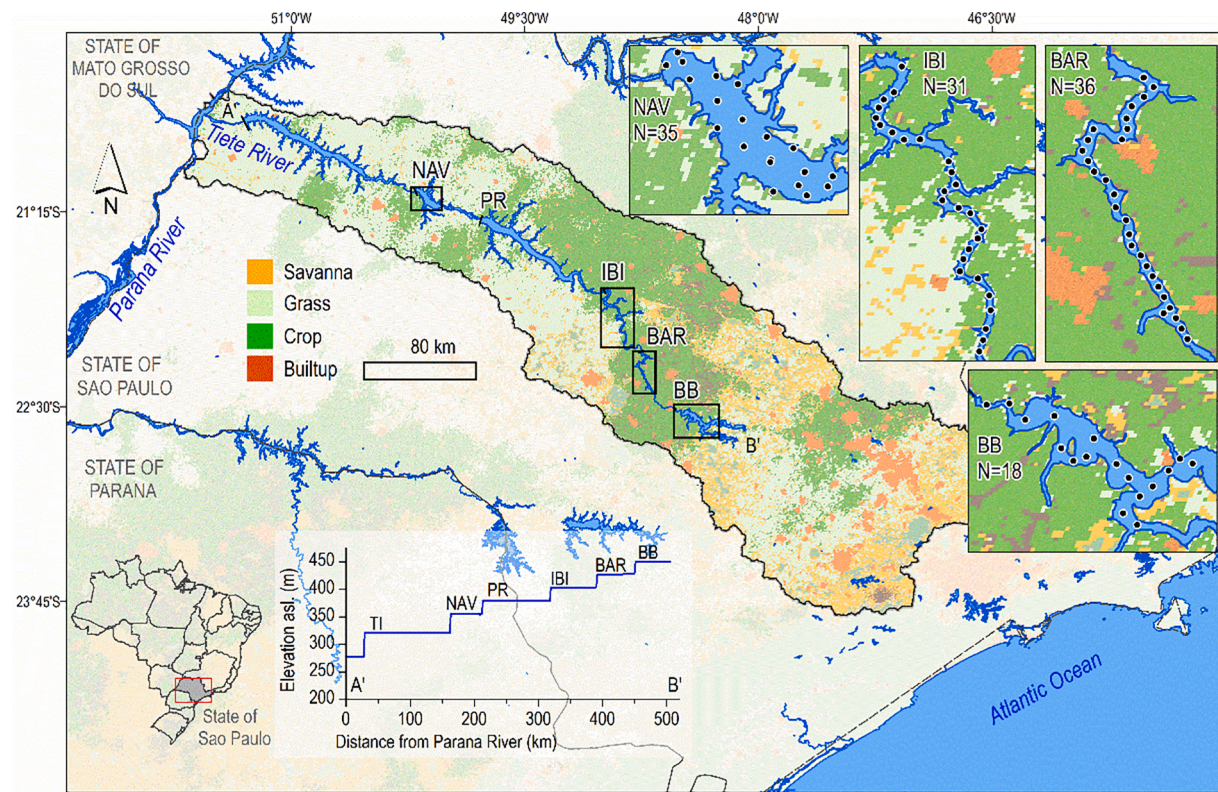


**Fig. 1.** Sampling points in the TRCS in the State of São Paulo. Reservoirs: Nova Avanhandava (NAV), Promissão (PR), Ibitinga (IBI), Bariri (BAR) and Barra Bonita (BB). The longitudinal profile calculated from the SRTM DEM along the Tietê River shows the reservoir cascades and impounded the water body with no slope. We used the MODIS-driven annual land cover product of 2019 (MCD12Q1 v006, 500 m) as a background layer with 45% transparency.

the model calibration: 18 sample points from BB, collected on May 5–9, 2014; 36 sample points from BAR, collected on August 15–18, 2016 and June 23–24, 2017; 31 sample points from IBI, collected on July 19–23, 2016 and June 21–22, 2017; and 35 sample points from NAV, collected between April 28 and May 2, 2016 and September 24–26, 2014.

The reservoirs of the Tietê river form a cascade system built since the late 1960s to meet the fast-growing energy demand of this highly populated region. These sequential dams modify the water retention time of continuous rivers and alter the water components from up-to-downstream (Barbosa et al., 1999). The water quality improves from the upstream (BB) to downstream of the Tietê cascade system (Smith et al., 2014; Bernardo et al., 2019b). The first reservoir (BB) is located in a transitional region between tropical and subtropical climate, with the dry period between May and October and the wet period between November and April (Watanabe et al., 2016). The reservoirs are currently used for power generation, navigation, fishing, water supply, irrigation, etc.

The Tietê River watershed has about 29 million inhabitants, and near the metropolitan regions of São Paulo and Campinas are located the majority of irregular effluents discharge. Thereby, the water flow in the Tietê system is insufficient to assimilate the effluent generated by the high population contingent (ANA, 2017). According to Smith et al. (2014), the Tietê River receives significant amount of nutrients (Nitrogen and Phosphorus) from fertilized soil mainly by sugar cane crops near the reservoirs. Bernardo (2019) verified that in upstream of the Tietê river watershed has high number of industrial as artificial areas, responsible for high levels of sewage discharges. Besides, agriculture and pasture were verified as the main economic activities in downstream regions.

The state is divided into several Water Resources Management Unit (UGRHI) (CETESB, 2017). BB is formed by the union of two rivers, Tietê river (lower tributary) and Piracicaba river (upper tributary). Thereby, BB integrates two, UGRHI-5 (Rio Piracicaba) and UGRHI-10 (Rio Tietê).

IBI and BAR are the smallest reservoirs in the cascade and they are located in the same management unit, UGRHI-13. PR is part of the UGRHI-16. Finally, NAV is located in UGRHI-19.

Each reservoir presents a combination of lentic and lotic characteristics. Thus, a better analysis can be made based on water retention time. The size (volume), operation (Storage or run-of-river) and need for water by the hydroelectric power plant can impact the water retention time in these aquatic systems. The retention time in BB is 37–137 days, in BAR is 7–24 days, in IBI is 12–43 days, in Promissão is 124–458 days, and in NAV is 32–119 days (Barbosa et al., 1999). The retention time is also influenced by weather and seasonal conditions. BB (volume of  $3,622 \times 10^6 \text{ m}^3$ ) and Promissão ( $7,408 \times 10^6 \text{ m}^3$ ) are storage reservoirs, and BAR ( $607 \times 10^6 \text{ m}^3$ ), IBI ( $981 \times 10^6 \text{ m}^3$ ) and NAV ( $2,720 \times 10^6 \text{ m}^3$ ) are run-of-river reservoirs (<https://www.aestiete.com.br/en/>).

## 2.2. Laboratory analysis

Chl- $\alpha$  concentration was determined through filtration of water samples collected *in situ* on Whatman GF/F filter (GE Healthcare, Chicago), with a pore size of 0.7  $\mu\text{m}$ , and method of Chl- $\alpha$  extraction in 90 acetone solution as proposed by Golterman et al. (1978).  $a_\phi$ ,  $a_{CDOM}$  and  $a_{NAP}$  also were estimated in the laboratory through water samples. To determine both  $a_\phi$  and  $a_{NAP}$ , we adopted the Reflectance-Transmittance method developed by Tassan and Ferrari (2002), Tassan and Ferrari (1998), Tassan and Ferrari (1995). Readings of reflectance and transmittance of the Whatman GF/F filters with retained material were done in a UV-VIS 2600 spectrophotometer (Shimadzu, Kyoto, Japan), with dual-beam mode and integrating sphere. In turn,  $a_{CDOM}$  was determined by using the method proposed by Bricaud et al. (1981). Water samples were filtered on polycarbonate filters (GE Healthcare, Chicago), with 0.2  $\mu\text{m}$  pore size, and absorbance measurements of water filtered were read in a UV-VIS 2600 spectrophotometer, with single beam mode, and 1 cm cuvette. Ultrapure water was used as a blank reference.

### 2.3. Radiometric data

Radiometric data (radiance and irradiance) were collected using TriOS/RAMSES (ACC-VIS and ARC-VIS) optical sensors (<http://www.trios.de>; Rastede, Germany). The sensors have 190 channels between 320 and 950 nm wavelength, and spectral sampling is at 3.3 nm with length accuracy of 0.3 nm. The viewing geometry of sensors was adopted accordingly to [Mobley \(1999\)](#) and the remote sensing reflectance ( $R_{rs}$ ) was calculated based equation:

$$R_{rs}(\theta, \varphi, \lambda) = \frac{L_t(\theta, \varphi, \lambda) - \rho \times L_{sky}(\theta, \varphi, \lambda)}{E_d(\lambda)} \quad (1)$$

where,  $L_t$  is the total radiance, which represents the sum between the water-leaving radiance ( $L_w$ ) and the surface-reflected radiance ( $L_r$ );  $L_{sky}$  is the sky radiance;  $\rho$  is defined as the ratio between  $L_t$  and  $L_{sky}$  from one direction, and  $E_d$  is the incident irradiance on the water surface. The  $R_{rs}$  was calculated as proposed by [Lee et al. \(2010\)](#), in which the spectral  $\rho$  variation was considered.

*In situ*  $R_{rs}$  data was resampled to represent OLI/Landsat-8 bands: B1 (Central  $\lambda = 443$ ), B2 (Central  $\lambda = 482$ ), B3 (Central  $\lambda = 561$ ) and B4 (Central  $\lambda = 655$ ). The relative spectral response of each OLI/Landsat 8 band ([Barsi et al., 2014](#)) was used to simulate the bands.

$$R_{rs}^{OLI} = \frac{\int_{\lambda_{min}}^{\lambda_{max}} R_{rs}(\lambda) \times S_{RF}(\lambda)}{\int_{\lambda_{min}}^{\lambda_{max}} S_{RF}(\lambda)} \quad (2)$$

where  $R_{rs}^{OLI}$  is the convoluted *in situ*  $R_{rs}$  for OLI bands;  $S_{RF}$  is the spectral response function for each band;  $\lambda_{max}$  and  $\lambda_{min}$  are the longer and shorter wavelengths in each band, respectively.

### 2.4. Quasi-Analytical Algorithm

The QAA ([Lee et al. 2002](#)) has provided satisfactory results in estimating the  $a_t$  and  $a_\phi$  in aquatic environments with different optical characteristics. We tested the QAA version 5 (QAA<sub>v5</sub>, [Lee et al., 2009](#)) and QAA<sub>TRCS</sub> ([Bernardo et al., 2019a](#)) to estimate the  $a_t$  and  $a_\phi$  from the study area. The QAA<sub>TRCS</sub> was parameterized to estimate the SPM concentration in the entire TRCS based on OLI/Landsat-8 bands. Reference wavelengths ( $\lambda_0$ ) are different for QAA<sub>v5</sub> ( $\lambda_0 = 560$  nm) and QAA<sub>TRCS</sub> ( $\lambda_0 = 655$  nm). [Bernardo et al. \(2019a\)](#) recommend the use of 5 or 2 as a multiplication factor in the denominator of  $\chi$ , depending on the turbidity of the environment. However, we decided to use only one value ( $\alpha = 5$ ), since the need for *a priori* turbidity information could hinder the systematic use of the proposed model in the future. Remote sensing reflectance below the water surface ( $r_{rs}$ ) was calculated following [Wang et al. \(2017\)](#).

The QAA requires the spectral band at 412 nm to retrieve the  $a_\phi$ , which OLI/Landsat-8 does not have. To overcome this limitation, we used the method proposed by [Wei et al. \(2019\)](#). These authors developed an algorithm to estimate the band at 412 nm from OLI bands B1, B2, B3 and B4. They assessed the model performance based on *in situ* measurements from different waters around the world, and it was found that the estimated band at 412 nm using their approach presented a median absolute percentage difference of ~9% ([Wei et al., 2019](#)).

### 2.5. Calibration of Chl-a model

We calibrated models to estimate Chl-a based on  $a_t$  and  $a_\phi$  by QAA<sub>v5</sub> and QAA<sub>TRCS</sub> from *in situ* radiometric data (Simulated OLI bands). Chl-a collected in the field campaigns were used in semi-analytical modeling. Least-square method was used to fit the relationship between  $a_t$  and  $a_\phi$  with Chl-a. The validation was conducted using the Leave-One-Out Cross Validation (LOOCV, [Arlot and Celisse, 2010](#); [Stone, 1974](#)). The accuracy assessment of Chl-a algorithms was performed using  $R^2$ , Root Mean Square Error (RMSE, Eq. (3)), Normalized RMSE (NRMSE, Eq.

(4)), Bias (Eq. (5)), and Nash–Sutcliffe model efficiency coefficient (NSE, Eq. (6)).

$$RMSE = \sqrt{\frac{\sum_{i=1}^n (y_i^E - y_i^M)^2}{n}} \quad (3)$$

$$NRMSE = \frac{RMSE}{y_{max} - y_{min}} \times 100 \quad (4)$$

$$Bias = \frac{\sum_{i=1}^n (y_i^E - y_i^M)}{n} \quad (5)$$

$$NSE = 1 - \frac{\sum_{i=1}^n (y_i^E - y_i^M)^2}{\sum_{i=1}^n (y_i^M - y_{average}^M)^2} \quad (6)$$

where,  $y_i^E$  is the estimated value for the  $i$  observation;  $y_i^M$  is the measured value for the  $i$  observation;  $y_{max}$  is the maximum measured value;  $y_{min}$  is the minimum measured value, and  $y_{average}^M$  is the average of measured values.

### 2.6. OLI/Landsat-8 selection and trophic state

The field campaigns carried out in IBI (July 19–23, 2016) and BAR (August 15–18, 2016) were used as a reference to select the OLI/Landsat-8 images. Three Landsat scenes were necessary to cover the entire study area. Although we did not collect field data from the Promissão reservoir (PR), Chl-a in this reservoir was also estimated because it is located in the same scene as IBI and BAR. It is also located between the two reservoirs with field data (IBI and NAV). Landsat-8 Level-2 products version 6 (Surface Reflectance) images of the selected dates were downloaded from the USGS Earth Explorer (<https://earthexplorer.usgs.gov/>). The first scene contained BB and it was acquired on July 30, 2016 (path 220 and row 76); the second scene contained IBI, BAR and PR, it was acquired on August 6, 2016 (path 221 and row 75); the NAV was contained in the last scene acquired on August 13, 2016 (path 222 and row 75). Those scenes were selected to be closest to the reference date (July–August 2016), as long as it did not contain clouds.

The QAA was applied for each pixel from the OLI images to obtain  $a_t$  and  $a_\phi$ . After that, the calibrated model with the highest performance was applied to the images with  $a$  values to retrieve the Chl-a concentration of the Tietê River reservoirs. Based on the Chl-a values, the trophic state of each reservoir was classified based on [Table 1](#).

## 3. Results and discussion

### 3.1. Spectral variability

The *in-situ* datasets of  $R_{rs}$  are shown in [Fig. 2](#). Different magnitudes through the  $R_{rs}$  spectra are largely caused by the varying concentration of OSCs. The green (500–600 nm) and NIR bands (>700 nm) are the ranges most sensitive to SPM. A high level of CDOM displaces the 550 nm- $R_{rs}$  peak toward 600 nm, as observed during the field surveys in BAR and IBI. A marked peak of  $R_{rs}$  near 550 nm is correlated with the

**Table 1**

Trophic state classification for reservoirs. Adapted from CETESB (2017).

Trophic classification	Chl-a (mg m <sup>-3</sup> )
Ultraoligotrophic	Chl-a ≤ 1.17
Oligotrophic	1.17 < Chl-a ≤ 3.24
Mesotrophic	3.24 < Chl-a ≤ 11.03
Eutrophic	11.03 < Chl-a ≤ 30.55
Supereutrophic	30.55 < Chl-a ≤ 69.05
Hypereutrophic	69.05 < Chl-a

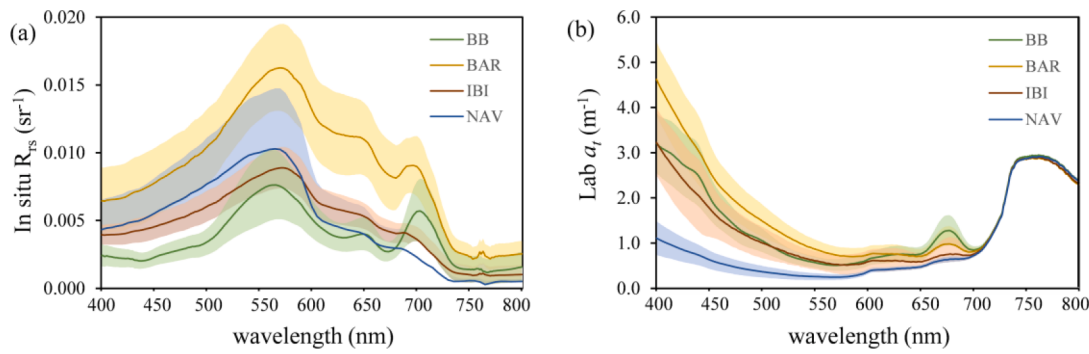


**Fig. 2.** *In situ R<sub>rs</sub>* and laboratory *a<sub>t</sub>* from sample points at BB, BAR, IBI and NAV.

relatively high SPM concentrations. A smaller peak around 650 nm in some curves also indicates the presence of phycocyanin, caused by the absorption feature near 620 nm and 670 nm, due to Chl-a (Gitelson, 1992).

### 3.2. QAA assessment

The band centered at 412 nm was used to retrieve *a<sub>φ</sub>* from QAA. The reflectance of this band (412 nm) was estimated based on OLI/Landsat-8 bands using the algorithm proposed by Wei et al. (2019). The validation for this approach is shown in Fig. 3.

The assessment of the QAA performance was conducted by comparing the estimated values by the QAA (TRCS and V5) at each bandwidth with the absorption values measured in the laboratory (Table 2).

In general, the *a<sub>t</sub>* values were better estimated using the QAA<sub>TRCS</sub>, whereas the QAA<sub>V5</sub> was better for estimating *a<sub>φ</sub>*. The band at 412 nm resulted in the lowest *a<sub>t</sub>* values, with NRMSE of 22.8% and 35.5% for QAA<sub>TRCS</sub> and QAA<sub>V5</sub>, respectively. The lowest *a<sub>φ</sub>* values were presented in the band at 561 nm, with NRMSE of 45% for QAA<sub>TRCS</sub> and 21.5% for QAA<sub>V5</sub>. NRMSE below 20% were shown for the four bands between 443 and 655 nm using QAA<sub>TRCS</sub> to estimate *a<sub>t</sub>*. NRMSE below 16% were presented for *a<sub>φ</sub>* using QAA<sub>V5</sub>, with the exception of the band at 561 nm.

### 3.3. Chl-a model calibration and validation

Table 3 shows the correlation (*r*) and the determination coefficient (*R*<sup>2</sup>) of linear and exponential models in estimating Chl-a based on the *a<sub>t</sub>*

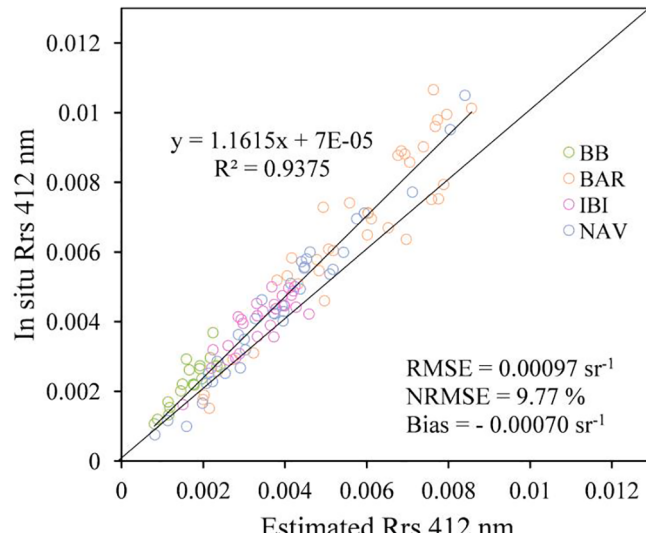


**Fig. 3.** Validation of the estimated band at 412 nm.

and *a<sub>φ</sub>* from QAA<sub>TRCS</sub> and QAA<sub>V5</sub>. In all cases, models based on *a<sub>t</sub>* or *a<sub>φ</sub>* (QAA<sub>TRCS</sub> or QAA<sub>V5</sub>) at 655 nm showed an excellent model fit, with *r* and *R*<sup>2</sup> for the linear regression greater than 0.787 and 0.619, respectively. This high correlation is related to the greater radiation absorption by the phytoplankton at the spectrum region near 655 nm. Although absorption around 482 nm is more related to the chlorophyll-*b*, absorption at 482 nm showed a high value of *r* (>0.77) and *R*<sup>2</sup> (>0.60) for both linear and exponential models, using both QAA<sub>TRCS</sub> or QAA<sub>V5</sub>.

It is worth mentioning that in order to retrieve the *a<sub>φ</sub>* through QAA, it is essential to estimate the reflectance at 412 nm, since OLI/Landsat sensor does not provide this band. Despite the high accuracy of this adopted procedure to interpolate the band at 412 nm (Fig. 3), this step may introduce uncertainties in the calibration process of modeling Chl-a. Hence, we decided to select a Chl-a model using the *a<sub>t</sub>*, since the band at 412 nm is not necessary to estimate *a<sub>t</sub>*, based on QAA. In addition, *r* and *R*<sup>2</sup> values of *a<sub>φ</sub>*, shown in Table 3, were not substantially higher than the values of *a<sub>t</sub>*. The QAA<sub>TRCS</sub> showed lower errors when estimating *a<sub>t</sub>* for all bands, in contrast to the QAA<sub>V5</sub>, as shown in Table 2. The *a<sub>t</sub>* (482 nm) and *a<sub>t</sub>* (655 nm) estimated by QAA<sub>TRCS</sub> (*a<sub>t</sub><sup>482</sup>* and *a<sub>t</sub><sup>655</sup>*, respectively) showed better results in estimating Chl-a from the TRCS (Table 3). The high correlation between Chl-a and *a<sub>t</sub><sup>482</sup>* and *a<sub>t</sub><sup>655</sup>* confirms that the phytoplankton absorbs much of the radiation near these regions of the spectrum. According to Gitelson (1992), there is strong absorption by both Chl-a and CDOM between 400 nm and 500 nm, and high absorption by Chl-a near 675 nm. Therefore, the Chl-a model based on both *a<sub>t</sub><sup>482</sup>* and *a<sub>t</sub><sup>655</sup>* using QAA<sub>TRCS</sub> was tested in this study (Fig. 4).

The linear model based on *a<sub>t</sub><sup>482</sup>* + *a<sub>t</sub><sup>655</sup>* (QAA<sub>TRCS</sub>) generated *R*<sup>2</sup> = 0.62. The exponential model based on *a<sub>t</sub><sup>482</sup>* + *a<sub>t</sub><sup>655</sup>* (QAA<sub>TRCS</sub>) showed promising results with *r* and *R*<sup>2</sup> of 0.790 and 0.646, respectively. Nevertheless, one issue with the linear model is that a reservoir with low *a<sub>t</sub>* (i.e., *a<sub>t</sub><sup>482</sup>* + *a<sub>t</sub><sup>655</sup>* lower than ~1.5 m<sup>-1</sup>), such as Nova Avanhandava, could result in negative values of Chl-a concentration (C, mg m<sup>-3</sup>). Therefore, the exponential model based on *a<sub>t</sub><sup>482</sup>* + *a<sub>t</sub><sup>655</sup>* (QAA<sub>TRCS</sub>) (Eq. (7)) was chosen to estimate the C from TRCS using OLI/Landsat-8. The error analysis results are shown in Table 4.

$$C = 0.2329e^{2.3341(a_t^{482} + a_t^{655})} \quad (7)$$

where C is the Chl-a concentration (mg m<sup>-3</sup>); *a<sub>t</sub><sup>482</sup>* (m<sup>-1</sup>) and *a<sub>t</sub><sup>655</sup>* (m<sup>-1</sup>) are total absorption coefficients at bands 482 nm and 655 nm based on QAA<sub>TRCS</sub>, respectively.

The Chl-a concentration estimated in this study resulted in a reasonable error, with NRMSE of 15.3%. A negative bias of 7.22 mg m<sup>-3</sup> was observed, i.e., indicating a slight underestimation in Chl-a values. The NSE based on all data points presented the best value (0.49), since NSE = 1 corresponds to a perfect agreement between observed and estimated data. The model validation for individual reservoirs showed a range of errors. NAV presented lower RMSE (4.2 mg m<sup>-3</sup>). It is known that NAV is a clear water reservoir with low Chl-a content (and thus low range); thereby, a small error in the Chl-a estimates from NAV can result

**Table 2**Error evaluation for  $a_t$  and  $a_\phi$  estimated by QAA<sub>TRCS</sub> and QAA<sub>V5</sub>.

$\lambda$ (nm)	$a_t$ QAA <sub>TRCS</sub>			$a_t$ QAA <sub>V5</sub>		
	RMSE ( $m^{-1}$ )	NRMSE (%)	BIAS ( $m^{-1}$ )	RMSE ( $m^{-1}$ )	NRMSE (%)	BIAS ( $m^{-1}$ )
412	1.242	22.8	-0.075	1.933	35.5	-0.583
443	0.837	19.6	-0.120	1.384	32.4	-0.572
482	0.436	17.0	-0.039	0.748	29.2	-0.495
561	0.190	15.2	0.004	0.292	23.2	-0.400
655	0.247	18.5	0.051	0.271	20.3	-0.253
$\lambda$ (nm)	$a_\phi$ QAA <sub>TRCS</sub>			$a_\phi$ QAA <sub>V5</sub>		
	RMSE ( $m^{-1}$ )	NRMSE (%)	BIAS ( $m^{-1}$ )	RMSE ( $m^{-1}$ )	NRMSE (%)	BIAS ( $m^{-1}$ )
412	0.494	15.5	-0.179	0.498	15.6	-0.420
443	0.506	15.6	-0.052	0.483	14.9	-0.333
482	0.347	28.2	0.847	0.188	15.3	0.262
561	0.249	45.0	1.911	0.119	21.5	0.816
655	0.275	21.9	0.560	0.192	15.3	-0.289

**Table 3**Comparison of linear (Lin) and exponential (Exp) models to estimate Chl-a using  $a_t$  and  $a_\phi$  from QAA<sub>TRCS</sub> and QAA<sub>V5</sub>.

$\lambda$ (nm)	$a_t$ QAA <sub>TRCS</sub>			$a_t$ QAA <sub>V5</sub>		
	r	R <sup>2</sup> (Lin)	R <sup>2</sup> (Exp)	r	R <sup>2</sup> (Lin)	R <sup>2</sup> (Exp)
412	0.729	0.532	0.484	0.741	0.549	0.496
443	0.760	0.578	0.546	0.768	0.589	0.543
482	0.776	0.602	0.640	0.805	0.648	0.638
561	0.417	0.174	0.309	0.720	0.518	0.604
655	0.798	0.637	0.577	0.787	0.619	0.521
$\lambda$ (nm)	$a_\phi$ QAA <sub>TRCS</sub>			$a_\phi$ QAA <sub>V5</sub>		
	r	R <sup>2</sup> (Lin)	R <sup>2</sup> (Exp)	r	R <sup>2</sup> (Lin)	R <sup>2</sup> (Exp)
412	0.639	0.408	0.387	0.728	0.530	0.509
443	0.630	0.397	0.379	0.726	0.527	0.509
482	0.491	0.241	0.301	0.760	0.577	0.613
561	0.060	0.004	0.043	0.640	0.410	0.540
655	0.788	0.620	0.564	0.787	0.619	0.520

in a significant relative error (NRMSE = 23.8%). BB presented the highest RMSE ( $80.2 \text{ mg m}^{-3}$ ), followed by BAR ( $48.7 \text{ mg m}^{-3}$ ), and IBI ( $23.5 \text{ mg m}^{-3}$ ). According to Alcântara et al. (2016c) the highest error observed for BB can be explained by the phytoplankton package effect, which is a physiological strategy for large phytoplankton species that reduces the absorption spectra. The Chl-a measured in the field (Y axis in Fig. 4) showed the decreasing values in the following order: BB, BAR, IBI and NAV. This indicates that the calibrated model may generate lower RMSE if the Chl-a range is low, and higher RMSE when the Chl-a range is high. Nevertheless, the NRMSE indicates the prospective applicability of our model with 20 and 30% for each reservoir.

### 3.4. Chl-a modeling and the spatial distribution

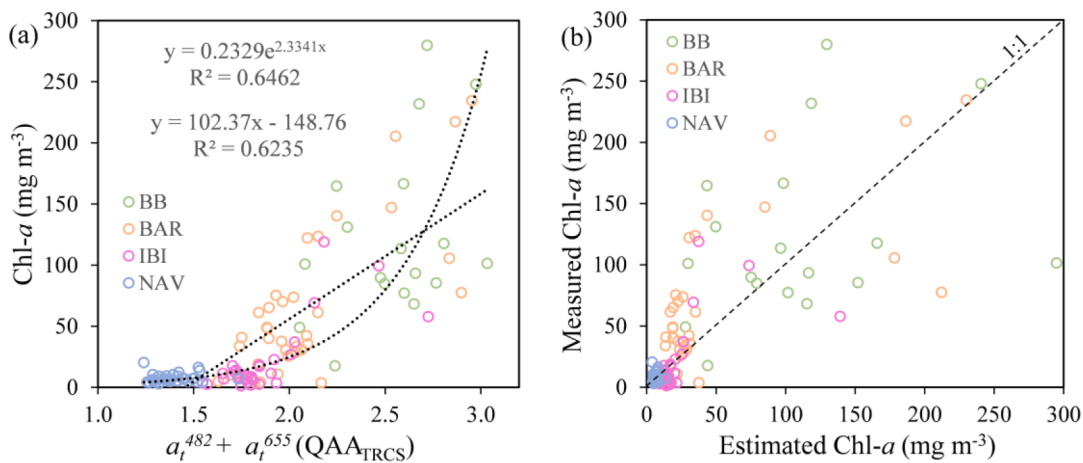
Field data were collected in the years 2014, 2016 and 2017. The campaigns dates and sampling points locations were defined based on Chl-a variability, in addition to considering meteorological factors and satellite image acquisition date. Thereby, field data varied from April to September. In this sense, we believe that it was possible to obtain representative data of Chl-a for the entire Tietê cascade under study, with values ranging from 1 to  $280 \text{ mg m}^{-3}$ .

The Tietê reservoirs (mainly those near to the biggest cities of São Paulo state, such as BB, IBI and BAR) can show high variation in Chl-a concentration. Between July 1993 and June 1994, the Chl-a in BB presented lowest value in March ( $7.4 \text{ mg m}^{-3}$ ) and highest value in April ( $438.0 \text{ mg m}^{-3}$ ) (Calijuri et al., 2002). In addition, Calijuri et al. (2002) observed in a single month (July) Chl-a ranging from  $7 \text{ mg m}^{-3}$  to  $187 \text{ mg m}^{-3}$ . In IBI, it was observed Chl-a variation between 3.0 and  $258.8 \text{ mg m}^{-3}$  (Cairo et al., 2020; Cairo, 2015). In BAR, Tundisi (1983) presented

**Table 4**

Error analysis from the model calibration based on Equation (7) to estimate C in Nova Avanhandava (NAV), Ibitinga (IBI), Bariri (BAR), Barra Bonita (BB) and all the four reservoirs (All data).

	RMSE ( $\text{mg m}^{-3}$ )	NRMSE (%)	Bias	NSE
All data	42.7	15.3%	-7.22	0.49
NAV	4.2	23.8%	-1.26	-0.32
IBI	23.5	19.9%	2.30	0.29
BAR	48.7	21.1%	-18.07	0.34
BB	80.2	30.6%	-13.53	-0.39

**Fig. 4.** Scatter plot showing linear and exponential fit between Chl-a and  $a_t$  QAA<sub>TRCS</sub> ( $a_t^{482} + a_t^{655}$ ) in (a) and measured vs. estimated Chl-a in (b) for the exponential model.

Chl-a of  $20.3 \text{ mg m}^{-3}$  on 1979, and Padisák et al. (2000) indicated a variation between 55 and  $77 \text{ mg m}^{-3}$  on 1998. PR and NAV have shown lower values of Chl-a, in addition to being more homogeneous over time. Variation of  $3\text{--}9 \text{ mg m}^{-3}$  was observed by Ferrareze (2012) between 2003 and 2004 in PR. Mallasen et al. (2012) found an average lower than  $6.0 \text{ mg m}^{-3}$  for three sampling stations in NAV between 2005 and 2007.

In the present work, we decided to select only one date (resulting in 3 OLI images to cover all study area) to estimate Chl-a and the trophic state of Tietê reservoirs. Only the 2016 field data from IBI and BAR match with the image. As the model to estimate Chl-a was calibrated based on  $a_t$ , the difference between satellite dates and field dates was not a problem, since we used an IOP. However, for a deeper assessment, a temporal analysis using the proposed methodology could be applied. Therefore, it is suggested, for future work, a temporal analysis of Chl-a in the Tietê cascade system based on our methodology.

Three Level-2 OLI/Landsat-8 images were selected to cover the entire TRCS in July/August 2016. QAAATRCS was used to retrieve  $a_t^{482}$  and  $a_t^{655}$  from those OLI images. The exponential model (Fig. 4) was used to estimate the Chl-a based on images  $a_t$  (Fig. 5). Chl-a concentration histograms for each reservoir were plotted to assess the result.

NAV (Fig. 5) presented a homogeneous pattern with low Chl-a concentration in the entire reservoir. Chl-a concentration ranged up to  $10 \text{ mg m}^{-3}$ . PR (Fig. 5), with a median of  $6 \text{ mg m}^{-3}$ , presented values up to  $\sim 15 \text{ mg m}^{-3}$ . In PR, the model was able to identify hotspots of Chl-a values upstream of the reservoir. These hotspots might be related to the phytoplankton inputs from IBI or from the small tributaries of the surrounding catchments. The waterbody with high Chl-a concentration close to the left bank of the river seemed to not mix effectively with the other waterbodies with relatively smaller Chl-a concentration. This leads it to remain as a "plume". A median of  $10 \text{ mg m}^{-3}$  was obtained for IBI (Fig. 5) and it was identified that some tributaries had Chl-a concentration between 15 and  $30 \text{ mg m}^{-3}$ , probably related to the nutrients and pollutants sourcing from the cattle ranching and built-up environments from the catchment that instantaneously triggered the algae blooms. The highest Chl-a median ( $13.7 \text{ mg m}^{-3}$ ) was observed in BAR (Fig. 5), with the values ranging from 10 to  $20 \text{ mg m}^{-3}$ . According to Gomes et al. (2020), the high Chl-a concentration and  $a_{CDOM}$  predominance in BAR suggest that there are multiple sources of organic matter for the reservoir. These might include meteorological conditions and waste from urban, industrial and agricultural areas. In BB (Fig. 5), the difference in concentration of Chl-a between the Piracicaba River (upper

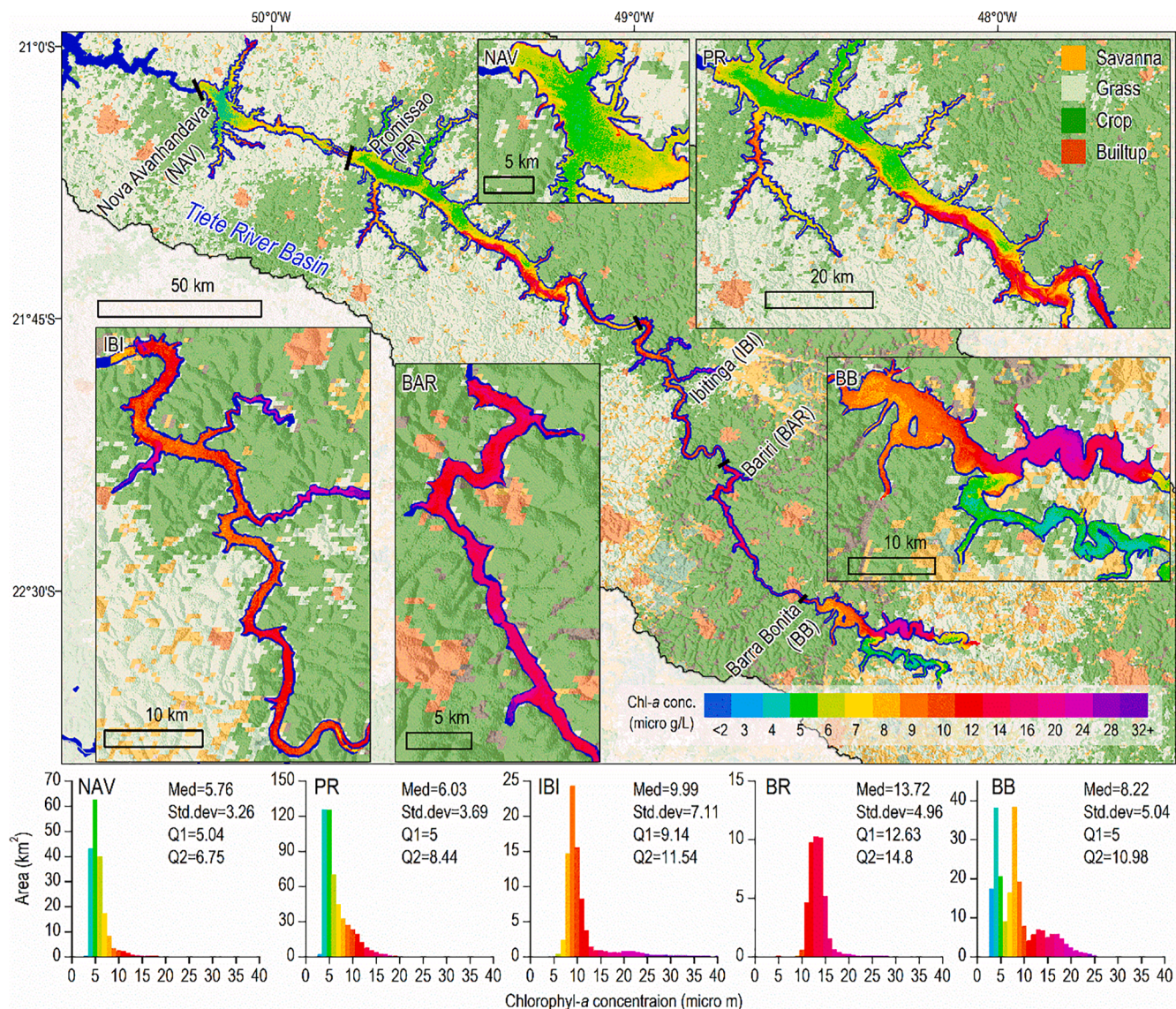


**Fig. 5.** Chl-a mapping and histogram from NAV (a), PR (b), IBI (c), BAR (d) and BB (e). OLI/Landsat-8 images acquired on July 30, 2016, for BB; August 6, 2016 for BAR, IBI and PR; and on August 13, 2016, for NAV.

tributary) and the Tietê River (lower tributary) is clearly captured. This difference is also observed in the histogram with the two high modes (near to 4 and 9 mg m<sup>-3</sup>) and another wider mode between 12 and 20 mg m<sup>-3</sup>. After the Tietê and Piracicaba rivers meet, the Chl-a concentration reaches intermediate and homogeneous values around 9 mg m<sup>-3</sup>. Other studies showed an underestimation of Chl-a concentration in the Tietê River before the confluence, although the content of this pigment has been high (Watanabe et al., 2019; 2015). For example, a sample point collected in the field with a value of 89 mg m<sup>-3</sup>, resulted in a value of 5 mg m<sup>-3</sup> based on the estimate with the satellite image. However, it is worth remembering that the field collection was carried out in May 2014 and the image was acquired in July 2016. Thus, internal and external factors from this aquatic system may have occurred to alter the concentration of Chl-a in this analyzed date. The high sewage load coming from the lower course of the Tietê River is responsible for the singular bio-optical status found in this section, which can have hindered the Chl-a modelling (Watanabe et al., 2017).

In general, most pixels across the retrieved images showed Chl-a values up to 30 mg m<sup>-3</sup>. However, when calibrating the model, we used several samples with values above 30 mg m<sup>-3</sup>, especially from BB and BAR. Thus, our model might underestimate the values in the reservoirs with high Chl-a values. However, a further assessment of the model's accuracy is hampered by the lack of OLI/Landsat images on the same day with the field campaign. However, our model was able to effectively estimate Chl-a concentration with relatively high accuracy and capture

their distribution showing the different patterns of the trophic status and hydrodynamic patterns between the reservoirs in the Tietê cascade.

Regarding the results of Chl-a shown in Fig. 5 and using Table 1, we determined the trophic state for each reservoir. The percentage of each trophic state class for each reservoir is shown in Fig. 6.

In most reservoirs, the predominance of the mesotrophic class was observed, with a significant percentage being eutrophic. BAR presented the worst trophic state, with almost 97% in eutrophic class. In general, the trophic state of the reservoirs was consistent with the result presented by São Paulo's State Sanitation Technology Company (CETESB) about trophic state analysis of inland waters quality for 2016 (CETESB, 2017). In 2016, the trophic status of São Paulo State was assessed from a total of 408 samples of Phosphorus and Chl-a. Most of these were sampled bimonthly and analyzed based on the 22 Water Resources Management Unit (UGRHI) (CETESB, 2017).

BB is divided in two hydrographic unit management: UGRHI-5 and UGRHI-10. According to CETESB (2017), from the 83 sample points at UGRHI-5, 32% were classified as eutrophic or worse and 68% as mesotrophic or better. In UGRHI-10 (24 sample points), 38% were classified as eutrophic or worse and 62% as mesotrophic or better. The trophic state of Barra Bonita presented in Fig. 6 (25% eutrophic and 75 mesotrophic) is in agreement with the report presented by CETESB (2017) for UGRHIs 5 and 10. IBI and BAR are located in the same management unit, UGRHI-13. According to CETESB (2017), from the 13 sample points of UGRHI-13 collected in 2016, 23% were classified as

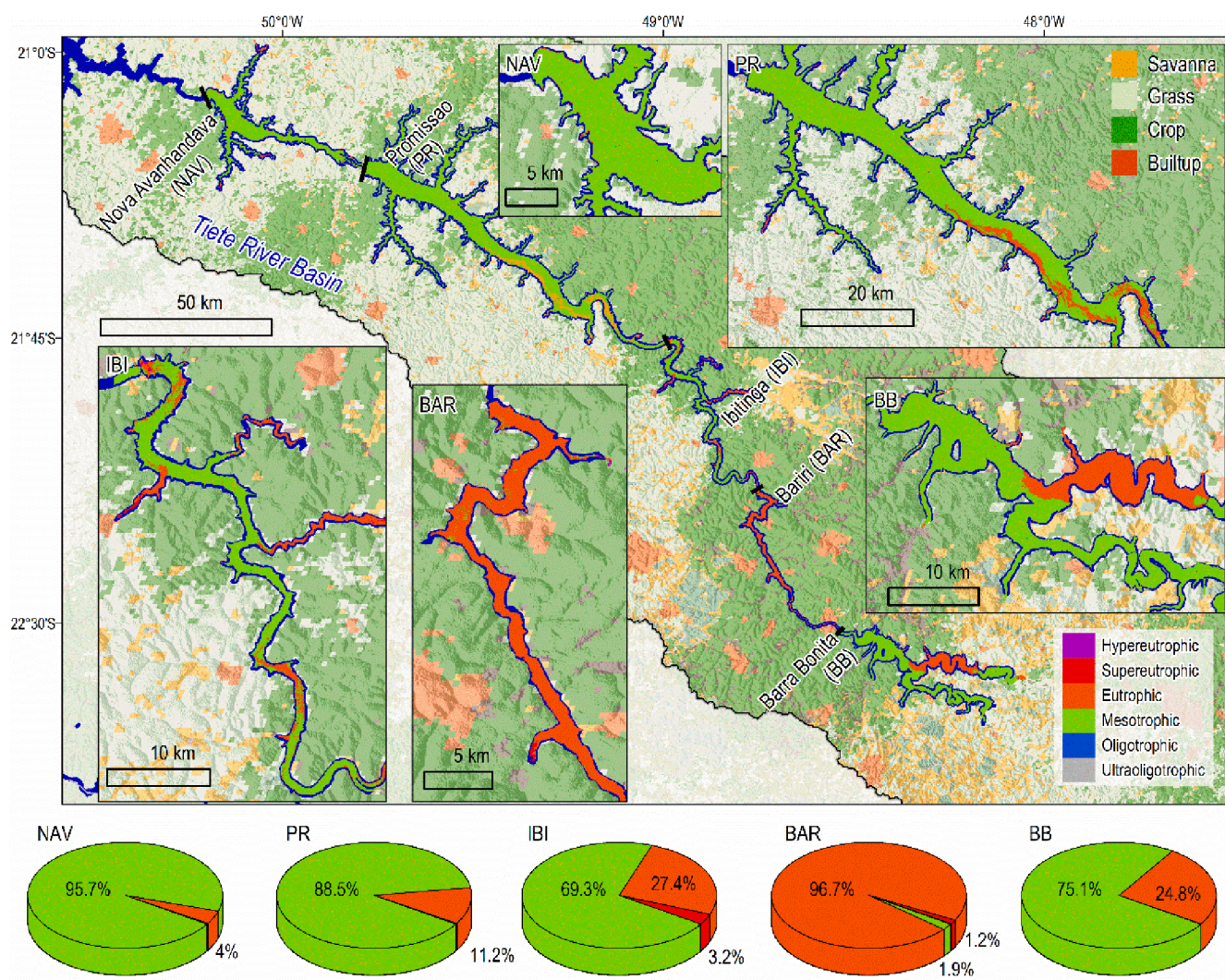


**Fig. 6.** Trophic status classification based on Chl-a map. Percentage of each trophic state class for each reservoir is indicated in pie chart.

oligotrophic, 62% as mesotrophic and 15% as eutrophic. Comparable trophic states were presented for IBI in Fig. 6, with 69.3% mesotrophic, 27.4% eutrophic and 3.2% supereutrophic. In BAR, a highly eutrophic status was observed, with 97% classified as eutrophic. PR and NAV are part of the UGRHI-16 and UGRHI-19, respectively. According to CETESB (2017), UGRHI-16 has 9 sample points, the vast majority (78%) are oligo or mesotrophic, and 22% eutrophic; in UGRHI-19 (with 11 sample points) all points were classified as ultraoligo, oligo or mesotrophic. NAV and PR presented a very similar trophic state (Fig. 6), where the vast majority of the pixels belong to the mesotrophic class. Furthermore, PR and NAV were in agreement when compared to the CETESB (2017).

Although in our work, the trophic state of the TRCS was assessed using the images acquired on a single date, using the Chl-a model developed in this study, it becomes possible to monitor the trophic state regularly, i.e. every 16 days in case of using the Landsat series. This study has, therefore, a great potential in contributing to the water quality management of TRCS by operationally reconstructing the Chl-a maps across the cascade enabling both the spatiotemporal assessment of the trophic status.

#### 4. Conclusion

In this study, we developed a semi-analytical model to estimate the Chl-a and assess its spatial distribution patterns in the TRCS, in Brazil. We used  $a_t$  instead of  $a_\phi$  to estimate Chl-a, and demonstrate that  $a_t$  values were better estimated using QAA<sub>TRCS</sub> than QAA<sub>V5</sub>, with NRMSE around 22.8%.  $a_t^{482}$  and  $a_t^{655}$  estimated by QAA<sub>TRCS</sub> presented a strong correlation with the Chl-a. This is mainly due to the phytoplankton absorbing radiation at wavelengths near to 482 nm and 655 nm for photosynthesis. So that, the exponential model based on  $a_t^{482} + a_t^{655}$  presented a satisfactory result whilst covering the entire data range, with  $R^2$  of 0.646 and NRMSE of 15.3%. The use of OLI/Landsat-8 images to retrieve  $a_t$  with basis in a single QAA to estimate Chl-a across the entire TRCS presented promising results. The next step is to apply the model over an image time series and evaluate its effectiveness. The use of more than one OLI scene, due to the large study area, was not a problem in estimating Chl-a. OLI together with the proposed model proved to be feasible to be applied for TRCS and could be used to perform temporal analysis.

Although the CETESB monitors the Chl-a concentration periodically through field sampling, it is often limited by the operational cost and dependent on weather conditions. And until now the trophic state of the TRCS has only been assessed partially since it is only based on a few point samples. For the first time, we provide the spatially distributed information on the trophic state across the entire reservoir cascade at a low cost, and we believe that this will become an efficient alternative to the conventional monitoring practices that can inform the reservoir managers for necessary actions such as to mitigate the environmental impacts caused by an algae bloom.

#### CRediT authorship contribution statement

**Luiz Rotta:** Conceptualization, Methodology, Formal analysis, Data curation, Writing - original draft. **Enner Alcântara:** Conceptualization, Methodology, Formal analysis, Writing - review & editing. **Edward Park:** Conceptualization, Methodology, Formal analysis, Writing - review & editing. **Nariâne Bernardo:** Data curation, Writing - review & editing. **Fernanda Watanabe:** Data curation, Writing - review & editing.

#### Declaration of Competing Interest

The authors declare that they have no known competing financial interests or personal relationships that could have appeared to influence the work reported in this paper.

#### Acknowledgement

E.A. acknowledge the São Paulo Research Foundation (FAPESP) under grant 19/00259-0. L.H.S.R acknowledges the Coordination for the Improvement of Higher Education Personnel – (CAPES) for the post-doctoral fellowship PNPD n° 88882.317841/2019-01. E.P. acknowledges the SUG-NAP (3/19 EP) grant at the Nanyang Technological University. The authors also thank Prof. Dr. Edivaldo D. Velini and the staff of School of Agriculture (UNESP/Botucatu) for allowing the use of their laboratory facilities.

#### References

- Abe, D.S., Sidagis-Galli, C., Tundisi, T.M., Tundisi, J.E.M., Grimberg, D.E., Medeiros, G.R., Teixeira-Silva, V., Tundisi, J.G., 2009. The effect of eutrophication on greenhouse gas emissions in three reservoirs of the Middle Tietê River, southeastern Brazil. SIL Proceedings, 1922–2010. 30 (6), 822–825. <https://doi.org/10.1080/03680770.2009.11902248>.
- AES Tieté, 2020. Website. <https://www.aestiete.com.br/en/> (accessed 5 May 2020).
- ANA, 2017. National Water Agency (Brazil). Atlas esgotos: despoluição de bacias hidrográficas. Agência Nacional de Águas /Secretaria Nacional de Saneamento Ambiental. Brasília: ANA.
- Alcântara, E., Bernardo, N., Watanabe, F.S.Y., Rodrigues, T., Rotta, L., Carmo, A.F.C., Shimabukuro, M., Gonçalves, S., Imai, N., 2016a. Estimating the CDOM absorption coefficient in tropical inland waters using OLI/Landsat-8 images. Remote Sensing Letters 7, 661–670. <https://doi.org/10.1080/2150704X.2016.1177242>.
- Alcântara, E., Marcelo Curtarelli, M., Stech, J., 2016b. Estimating total suspended matter using the particle backscattering coefficient: results from the Itumbiara hydroelectric reservoir (Goiás State, Brazil). Remote Sensing Letters 7 (4), 397–406. <https://doi.org/10.1080/2150704X.2015.1137646>.
- Alcântara, E., Watanabe, F., Rodrigues, T., Bernardo, N., 2016c. An investigation into the phytoplankton package effect on the chlorophyll-a specific absorption coefficient in Barra Bonita reservoir, Brazil. Remote Sensing Letters 7 (8), 761–770. <https://doi.org/10.1080/2150704X.2016.1185189>.
- Andrade, C.P., Alcantara, E.H., Bernardo, N., Kampel, M., 2019. An assessment of semi-analytical models based on the absorption coefficient in retrieving the chlorophyll-a concentration from a reservoir. Advances in Space Research 63, 2175–2188. <https://doi.org/10.1016/j.asr.2018.12.023>.
- Arlot, S., Celisse, A., 2010. A survey of cross-validation procedures for model selection. Stat. Surv. 2010 (4), 40–79. <https://doi.org/10.1214/09-SS054>.
- Barbosa, F.A.R., Padisák, J., Espíndola, E.L.G., Borics, G., Rocha, O., 1999. The cascading reservoir continuum concept (CRCC) and its application to the river Tietê-basin, São Paulo State, Brazil. Theoretical Reservoir Ecology and its Applications 425–437.
- Barsi, J.A., Lee, K., Kvaran, G., Markham, B.L., Pedelty, J.A., 2014. The spectral response of the Landsat-8 operational land imager. Remote Sensing 6, 10232–10251. <https://doi.org/10.3390/rs61010232>.
- Bernardo, N., 2019. A semianalytical algorithm to retrieve the suspended particulate matter in a cascade reservoir system with widely differing optical properties. Doctoral thesis. Postgraduate program in cartographic sciences - São Paulo State University. Presidente Prudente/SP, Unesp, Brazil.
- Bernardo, N., Alcântara, E., Watanabe, F., Rodrigues, T., Carmo, A.D., Gomes, A.C.C., Andrade, C., 2019b. Light absorption budget in a reservoir cascade system with widely differing optical properties. Water 11 (2), 229. <https://doi.org/10.3390/w11020229>.
- Bernardo, N., Carmo, A., Park, E., Alcântara, E., 2019a. Retrieval of suspended particulate matter in inland waters with widely differing optical properties using a semi-analytical scheme. Remote Sensing 11 (19), 2283. <https://doi.org/10.3390/rs11192283>.
- Bernardo, N., Watanabe, F.S.Y., Rodrigues, T.W.P., Alcântara, E., 2016. Evaluation of the suitability of MODIS, OLCI and OLI for mapping the distribution of total suspended matter in the Barra Bonita Reservoir (Tietê River, Brazil). Remote Sensing Applications: Society and Environment 4, 68–82. <https://doi.org/10.1016/j.rsase.2016.06.002>.
- Bohn, V.Y., Carmona, F., Rivas, R., Lagomarsino, L., Diovisalvi, N., Zagarese, H.E., 2018. Development of an empirical model for chlorophyll-a and Secchi Disk Depth estimation for a Pampean shallow lake (Argentina). The Egyptian Journal of Remote Sensing and Space Science 21 (2), 183–191. <https://doi.org/10.1016/j.ejrrss.2017.04.005>.
- Bricaud, A., Morel, A., Prieur, L., 1981. Absorption by dissolved organic matter of the sea (yellow substance) in the UV and visible domains. Limnology and Oceanography 26, 43–53. <https://doi.org/10.4319/lo.1981.26.1.0043>.
- Cairo, C., Barbosa, C., Lobo, F., Novo, E., Carlos, F., Maciel, D., Flores Júnior, R., Silva, E., Curtarelli, V., 2020. Hybrid chlorophyll-a algorithm for assessing trophic states of a tropical Brazilian reservoir based on MSI/Sentinel-2 data. Remote Sensing 12 (1), 40. <https://doi.org/10.3390/rs12010040>.
- Cairo, C.T., 2015. Temporal characterization of the bio-optical properties of the Ibitinga/SP reservoir. Master's Thesis, National Institute for Space Research (INPE), São José dos Campos/SP, Brazil. <http://urlib.net/8JMKD3MGP3W34P/3J4KK5E>.
- Calijuri, M.D.C., Dos Santos, A.C.A., Jati, S., 2002. Temporal changes in the phytoplankton community structure in a tropical and eutrophic reservoir (Barra Bonita, SP—Brazil). Journal of Plankton Research 24 (7), 617–634. <https://doi.org/10.1093/plankt/24.7.617>.

- CETESB – Companhia Ambiental do Estado de São Paulo, 2017. Qualidade das águas interiores no estado de São Paulo - 2016. <https://cetesb.sp.gov.br/aguas-interiores/publicacoes-e-relatorios/> (accessed 1 April 2020).
- Dall'Olmo, G., Gitelson, A.A., 2005. Effect of bio-optical parameter variability on the remote estimation of chlorophyll-a concentration in turbid productive waters: experimental results. *Applied Optics* 44, 412–422. <https://doi.org/10.1364/AO.44.000412>.
- Duan, H., Ma, R., Xu, J., Zhang, Y., Zhang, B., 2010. Comparison of different semi-empirical algorithms to estimate chlorophyll-a concentration in inland lake water. *Environmental Monitoring and Assessment* 170, 231–244. <https://doi.org/10.1007/s10661-009-1228-7>.
- Ferrareze, M., 2012. The effect of the land use on phytoplankton assemblages of a Cerrado stream (Brazil). *Acta Limnologica Brasiliensis* 24 (1), 43–51. <https://doi.org/10.1590/S2179-975X2012005000025>.
- FURNAS – Eletrobras Company. Website. 2020. <https://www.furnas.com.br/?culturae-en> (accessed 5 May 2020).
- Gitelson, A., 1992. The peak near 700 nm on radiance spectra of algae and water: relationships of its magnitude and position with chlorophyll concentration. *International Journal of Remote Sensing* 13, 3367–3373. <https://doi.org/10.1080/01431169208904125>.
- Gitelson, A.A., Dall'Olmo, G., Moses, W., Rundquist, D.C., Barrow, T., Fisher, T.R., Gurlin, D., Holz, J., 2008. A simple semi-analytical model for remote estimation of chlorophyll-a in turbid waters: validation. *Remote Sensing of Environment* 112 (9), 3582–3593. <https://doi.org/10.1016/j.rse.2008.04.015>.
- Golterman, H.L., Clymo, R.S., Ohnstad, M.A.M., 1978. Methods for Physical and Chemical Analysis of Freshwater. Blackwell Scientific Publications, Oxford. <https://doi.org/10.1002/iroh.19800650113>.
- Gomes, A.C., Alcântara, E., Rodrigues, T., Bernardo, N., 2020. Satellite estimates of euphotic zone and Secchi disk depths in a colored dissolved organic matter-dominated inland water. *Ecological Indicators* 110, 105848. <https://doi.org/10.1016/j.ecolind.2019.105848>.
- He, G., Fang, H., Bai, S., Liu, X., Chen, M., Bai, J., 2011. Application of a three-dimensional eutrophication model for the Beijing Guanting Reservoir, China. *Ecological Modelling* 222 (8), 1491–1501. <https://doi.org/10.1016/j.ecolmodel.2010.12.006>.
- Kallio, K., Koponen, S., Pulliaiainen, J., 2003. Feasibility of airborne imaging spectrometry for lake monitoring—a case study of spatial chlorophyll distribution in two meso-eutrophic lakes. *International Journal of Remote Sensing* 24 (19), 3771–3790. <https://doi.org/10.1080/0143116021000023899>.
- Karadžić, V., Subakov-Simić, G., Krizmanić, J., Natić, D., 2010. Phytoplankton and eutrophication development in the water supply reservoirs Garasi and Bokulja (Serbia). *Desalination* 255 (1–3), 91–96. <https://doi.org/10.1016/j.desal.2010.01.009>.
- Kim, B., Park, J.-H., Hwang, G., Jun, M.-S., Choi, K., 2001. Eutrophication of reservoirs in South Korea. *Limnology* 2 (3), 223–229. <https://doi.org/10.1007/s10201-001-8040-6>.
- Kirk, J.T., 2011. Light and Photosynthesis in Aquatic Ecosystems, third ed. Cambridge University Press.
- Le, C.F., Li, Y.M., Zha, Y., Sun, D., Yin, B., 2009. Validation of a quasi-analytical algorithm for highly turbid eutrophic water of Meiliang Bay in Taihu Lake, China. *IEEE Transactions on Geoscience and Remote Sensing* 47 (8), 2492–2500. <https://doi.org/10.1109/tgrs.2009.2015658>.
- Le, C.F., Hu, C., Cannizzaro, J., English, D., Muller-Karger, F., Lee, Z.P., 2013. Evaluation of chlorophyll-a remote sensing algorithms for an optically complex estuary. *Remote Sensing of Environment* 129, 75–89. <https://doi.org/10.1016/j.rse.2012.11.001>.
- Lee, Z.P., Ahn, Y., Mobley, C., Arnone, R., et al., 2010. Removal of surface-reflected light for the measurements of remote-sensing reflectance from an above-surface platform. *Opt. Express* 18 (25), 26313–26324. <https://doi.org/10.1364/OE.18.026313>.
- Lee, Z.P., Carder, K.L., Arnone, R.A., 2002. Deriving inherent optical properties from water color: a multiband quasi-analytical algorithm for optically deep waters. *Applied Optics* 41, 5755–5772. <https://doi.org/10.1364/AO.41.005755>.
- Lee, Z.P., Lubac, B., Werdell, J., Arnone, R., 2009. An Update of the Quasi-analytical Algorithm (QAA\_v5). IOC/CGG [http://www.iocccg.org/groups/Software\\_OCA/QAA\\_v5.pdf](http://www.iocccg.org/groups/Software_OCA/QAA_v5.pdf).
- Lee, Z.P., Shang, S., Qi, L., Yan, J., Lin, G., 2016. A semi-analytical scheme to estimate Secchi-disk depth from Landsat-8 measurements. *Remote Sensing of Environment* 177, 101–106. <https://doi.org/10.1016/j.rse.2016.02.033>.
- Li, L., Song, K., Li, Y., Tedesco, L.P., Shi, K., Li, Z., 2013. An inversion model for deriving optical properties validation and application. *Remote Sensing of Environment* 135, 150–166. <https://doi.org/10.1016/j.rse.2013.03.031>.
- Mallasen, M., de Barros, H.P., Traficante, D.P., Camargo, A.L.S., 2012. Influence of a net cage tilapia culture on the water quality of the Nova Avanhandava reservoir, São Paulo State, Brazil. *Acta Scientiarum. Biological Sciences* 34 (3), 289–296. <https://doi.org/10.4025/actascibiolsci.v34i3.7298>.
- Mishra, S., Mishra, D.R., 2012. Normalized difference chlorophyll index: a novel model for remote estimation of chlorophyll-a concentration in turbid productive waters. *Remote Sensing of Environment* 117, 394–406. <https://doi.org/10.1016/j.rse.2011.10.016>.
- Mishra, S., Mishra, D.R., Lee, Z.P., 2014. Bio-optical inversion in highly turbid and cyanobacteria-dominated waters. *IEEE Transactions on Geoscience and Remote Sensing* 52 (1), 375–388. <https://doi.org/10.1109/TGRS.2013.2240462>.
- Mobley, C.D., 1999. Estimation of the remote-sensing reflectance from above-surface measurements. *Applied Optics* 38 (36), 7442–7455. <https://doi.org/10.1364/AO.38.007442>.
- Oki, K., Yasuoka, Y., 2002. Estimation of chlorophyll concentration in lakes and inland seas with a field spectroradiometer above the water surface. *Applied Optics* 41 (30), 6463. <https://doi.org/10.1364/ao.41.006463>.
- Padisák, J., Barbosa, F.A.R., Borbély, G., Borics, G., Chorus, I., Espindola, E.L.G., Heinze, R., Rocha, O., Törökne, A.K., Vasas, G., 2000. Phytoplankton composition, biodiversity and a pilot survey of toxic cyanoprokaryotes in a large cascading reservoir system (Tietê basin, Brazil). *Internationale Vereinigung für theoretische und angewandte Limnologie: Verhandlungen* 27 (5), 2734–2742. <https://doi.org/10.1080/03680770.1998.11898164>.
- Rodgher, S., Espíndola, E.L.G., Rocha, O., Fracácia, R., Pereira, R.H.G., Rodrigues, M.H. S., 2005. Limnological and ecotoxicological studies in the cascade of reservoirs in the Tietê river (São Paulo, Brazil). *Brazilian Journal of Biology* 65 (4), 697–710. <https://doi.org/10.1590/s1519-69842005000400017>.
- Rodrigues, T., Alcantara, E., Rotta, L., Bernardo, N., Watanabe, F., 2020. An investigation into the relationship between light absorption budget and trophic status in inland waters. *Ecological Indicators* 115, 106410. <https://doi.org/10.1016/j.ecolind.2020.106410>.
- Rodrigues, T., Alcântara, E., Watanabe, F., Imai, N., 2017b. Retrieval of Secchi disk depth from a reservoir using a semi-analytical scheme. *Remote Sensing of Environment* 198, 213–228. <https://doi.org/10.1016/j.rse.2017.06.018>.
- Rodrigues, T., Guimaraes, U.S., Galo, M.L.T., 2014. Change detection as support for monitoring the dynamic of land around reservoir. In: 2014 IEEE Geoscience and Remote Sensing Symposium. <https://doi.org/10.1109/igarss.2014.6947421>.
- Rodrigues, T., Mishra, D.R., Alcântara, E., Astuti, I., Watanabe, F., Imai, N., 2018. Estimating the Optical Properties of Inorganic Matter-Dominated Oligo-to-Mesotrophic Inland Waters. *Water* 10, 449. <https://doi.org/10.3390/w10040449>.
- Rodrigues, T., Mishra, D.R., Alcantara, E., Watanabe, F., Rotta, L., Imai, N.N., 2017a. Retrieving total suspended matter in tropical reservoirs within a cascade system with widely differing optical properties. *IEEE Journal of Selected Topics in Applied Earth Observations and Remote Sensing* 10, 1–18. <https://doi.org/10.1109/JSTARS.2017.2745700>.
- Rotta, L.H.S., Mishra, D.R., Alcantara, E., Imai, N.N., Watanabe, F., Rodrigues, T., 2019. Kd(PAR) and a depth based model to estimate the height of submerged aquatic vegetation in an oligotrophic reservoir: a case study at Nova Avanhandava. *Remote Sensing* 11, 317. <https://doi.org/10.3390/rs11030317>.
- Rotta, L.H.S., Mishra, D.R., Watanabe, F., Rodrigues, T., Alcantara, E., Imai, N.N., 2018. Analyzing the feasibility of a space-borne sensor (SPOT-6) to estimate the height of submerged aquatic vegetation (SAV) in inland waters. *ISPRS Journal Of Photogrammetry And Remote Sensing* 144, 341–356. <https://doi.org/10.1016/j.isprsjprs.2018.07.011>.
- Smith, V.H., Tilman, G.D., Nekola, J.C., 1999. Eutrophication: impacts of excess nutrient inputs on freshwater, marine, and terrestrial ecosystems. *Environmental Pollution* 100 (1–3), 179–196. [https://doi.org/10.1016/s0269-7491\(99\)00091-3](https://doi.org/10.1016/s0269-7491(99)00091-3).
- Smith, W.S., Espíndola, E.L.G., Rocha, O., 2014. Environmental gradient in reservoirs of the medium and low Tietê River: limnological differences through the habitat sequence. *Acta Limnologica Brasiliensis* 26 (1), 73–88. <https://doi.org/10.1590/S2179-975X2014000100009>.
- Soares, J.S., Rocha, F.R., Fávaro, D.I.T., 2017. Metal and trace element concentration evaluation in sediment profiles of the Tietê River, state of São Paulo, by INAA and ICP OES techniques. In: International Nuclear Atlantic Conference - INAC, 2017, Belo Horizonte, MG. [http://inis.iae.org/collection/NCLCollectionStore\\_Public/49/015/49015703.pdf](http://inis.iae.org/collection/NCLCollectionStore_Public/49/015/49015703.pdf).
- Stone, M., 1974. Cross-validatory choice and assessment of statistical predictions. *Journal of the Royal Statistical Society: Series B (Methodological)* 36, 111–147. <https://doi.org/10.1111/j.2517-6161.1974.tb0094x>.
- Tassan, S., Ferrari, G.M., 1995. An alternative approach to absorption measurements of aquatic particles retained on filters. *Limnology and Oceanography* 40, 1358–1368. <https://doi.org/10.4319/lo.1995.40.8.1358>.
- Tassan, S., Ferrari, G.M., 1998. Measurement of light absorption by aquatic particles retained on filters: Determination of the optical pathlength amplification by the ‘transmittance-reflectance’ method. *Journal of Plankton Research* 20, 1699–1709. <https://doi.org/10.1093/plankt/20.9.1699>.
- Tassan, S., Ferrari, G.M., 2002. A sensitivity analysis of the ‘transmittance-reflectance’ method for measuring light absorption by aquatic particles. *Journal of Plankton Research* 24, 757–774. <https://doi.org/10.1093/plankt/24.8.757>.
- Tundisi, J.G., 1983. A review of basic ecological processes interacting with production and standing-stock of phytoplankton in lakes and reservoirs in Brazil. *Hydrobiologia* 100 (1), 223–243. <https://doi.org/10.1007/BF0027431>.
- Tundisi, J.G., Matsumura-Tundisi, T., Caljuri, M.C., Novo, E.M.L., 1991. Comparative limnology of five reservoirs in the middle Tietê River, São Paulo State. *Internationale Vereinigung für theoretische und angewandte Limnologie: Verhandlungen* 24 (3), 1489–1496. <https://doi.org/10.1080/03680770.1989.11899007>.
- Tundisi, J.G., Matsumura-Tundisi, T., Abe, D.S., 2008. The ecological dynamics of Barra Bonita (Tietê River, SP, Brazil) reservoir: implications for its biodiversity. *Brazilian Journal of Biology*, 68 (Suppl.), 1079–1098. <https://doi.org/10.1590/S1519-69842008000500015>.
- Tundisi, J.G., Matsumura-Tundisi, T., Caljuri, M.C., 1993. Limnology and management of reservoirs in Brazil. *Comparative Reservoir Limnology and Water Quality Management* 25–55. [https://doi.org/10.1007/978-94-017-1096-1\\_2](https://doi.org/10.1007/978-94-017-1096-1_2).
- Ussami, K.A., Guilhoto, J.J.M., 2018. Economic and water dependence among regions: the case of Alto Tietê, São Paulo State, Brazil. *Economia* 19 (3), 350–376. <https://doi.org/10.1016/j.econ.2018.06.001>.
- Wang, Y.W., Shen, F., Sokoletsy, L., Sun, X., 2017. Validation and Calibration of QAA Algorithm for CDOM Absorption Retrieval in the Changjiang (Yangtze) Estuarine and Coastal Waters. *Remote Sensing* 9, 1192. <https://doi.org/10.3390/rs9111192>.

- Watanabe, F.S.Y., Alcantara, E., Bernardo, N., Andrade, C.P., Gomes, A.C.C., Carmo, A.F.C., Rodrigues, T.W.P., Rotta, L.H.S., 2019. Mapping the chlorophyll-a horizontal gradient in a cascading reservoirs system using MSI Sentinel-2A images. *Advances In Space Research* 64, 581–590. <https://doi.org/10.1016/j.asr.2019.04.035>.
- Watanabe, F.S.Y., Alcantara, E., Curtarelli, M., Kampel, M., Stech, J., 2018. Landsat-based remote sensing of the colored dissolved organic matter absorption coefficient in a tropical oligotrophic reservoir. *Remote Sensing Applications: Society and Environment* 9, 82–90. <https://doi.org/10.1016/j.rsase.2017.12.004>.
- Watanabe, F.S.Y., Alcantara, E., Rodrigues, T., Imai, N.N., Barbosa, C.C.F., Rotta, L.H.S., 2015. Estimation of chlorophyll-a concentration and the trophic state of the Barra Bonita hydroelectric reservoir using OLI/Landsat-8 images. *International Journal of Environmental Research and Public Health* 2015 (12), 10391–10417. <https://doi.org/10.3390/ijerph120910391>.
- Watanabe, F.S.Y., Alcantara, E., Rodrigues, T., Rotta, L., Bernardo, N., Imai, N., 2017. Remote sensing of the chlorophyll-a based on OLI/Landsat-8 and MSI/Sentinel-2A (Barra Bonita reservoir, Brazil). *Anais da Academia Brasileira de Ciências*, 90 (2, Suppl. 1), 1987–2000. <https://doi.org/10.1590/0001-3765201720170125>.
- Watanabe, F.S.Y., Mishra, D.R., Astuti, I., Rodrigues, T., Alcantara, E., Imai, N., Barbosa, C., 2016. Parametrization and calibration of quasi-analytical algorithm for tropical eutrophic waters. *ISPRS Journal of Photogrammetry and Remote Sensing* 121, 28–47. <https://doi.org/10.1016/j.isprsjprs.2016.08.009>.
- Wei, J., Lee, Z.P., Shang, S., Yu, X., 2019. Semianalytical derivation of phytoplankton, CDOM, and detritus absorption coefficients from the Landsat 8/OLI reflectance in coastal waters. *Journal of Geophysical Research: Oceans* 124, 3682–3699. <https://doi.org/10.1029/2019JC015125>.
- Yoon, J-E., Lim, J-H., Son, S., Youn, S-H., Oh, H-J., Hwang, J-D., Kwon, J-I., Kim, S-S., Kim, I-N., 2019. Assessment of Satellite-Based Chlorophyll-a Algorithms in Eutrophic Korean Coastal Waters: Jinhae Bay Case Study. *Frontiers in Marine Science* 6, 359. <https://doi.org/10.3389/fmars.2019.00359>.
- Zhang, Y., Liu, M., Qin, B., van der Woerd, H.J., Li, J., Li, Y., 2009. Modeling remote-sensing reflectance and retrieving Chlorophyll-a concentration in extremely turbid Case-2 waters (Lake Taihu, China). *IEEE Transactions on Geoscience and Remote Sensing* 47 (7), 1937–1948. <https://doi.org/10.1109/TGRS.2008.2011892>.
- Zhang, Y., Ma, R., Duan, H., Loiselle, S., Zhang, M., Xu, J., 2016. A novel MODIS algorithm to estimate chlorophyll-a concentration in eutrophic turbid lakes. *Ecological Indicators* 69, 138–151. <https://doi.org/10.1016/j.ecolind.2016.04.020>.